Available online at www.sciencedirect.com
ScienceDirect
Journal of Photochemistry and Photobiology A: Chemistry 194 (2008) 111–121
Journal of Photochemistry and Photobiology A:Chemistry
www.elsevier.com/locate/jphotochem

Spectroscopic and calorimetric studies on the binding of the phototoxic and cytotoxic plant alkaloid sanguinarine with double helical poly(A)

Prabal Giri, Gopinatha Suresh Kumar *

Biophysical Chemistry Laboratory, Indian Institute of Chemical Biology, Kolkata 700032, India

Received 30 April 2007; received in revised form 9 July 2007; accepted 25 July 2007
Available online 31 July 2007

Abstract

The interaction of the phototoxic and cytotoxic DNA binding plant alkaloid sanguinarine with double stranded polyadenylic acid has been investigated from multifaceted spectroscopic and calorimetric techniques. The hypochromic and bathochromic shifts in the absorption spectrum, and large enhancement of the fluorescence intensity of sanguinarine indicated strong binding of the alkaloid to the duplex poly(A). The corresponding intrinsic binding constant for the complexation, obtained from visible absorbance and fluorescence spectroscopic methods, respectively, was found to be in the order of $10^4\ M^{-1}$. The binding was further characterized by strong energy transfer from the adenine base pairs to the alkaloid, significant polarization of the fluorescence of the alkaloid, stabilization against thermal strand separation of the duplex, and also resulting in remarkable conformational changes in poly(A) with concomitant generation of optical activity in the bound alkaloid molecules that are otherwise achiral. Isothermal titration calorimetric and differential scanning calorimetric studies revealed the binding of the alkaloid to be exothermic and enthalpy driven. All these results together with fluorescence quenching experiments advance good evidence for the intercalation of the alkaloid sanguinarine into the duplex poly(A).

Keywords: Sanguinarine; Polyriboadenylic acid; Binding; Energy transfer; Thermodynamics; Intercalation

1. Introduction

In contrast to the large number of studies on the mechanism of binding of drugs to DNA [1–7] studies on the interaction of small molecules with RNA are scanty. RNA plays crucial role in many key biological processes as well as in the progression of parasites and viruses and therefore its role as a prime target for therapeutic intervention has been acknowledged now [8–11]. The recent discovery of a variety micro RNAs further signifies the critical roles of RNA in life process [12–15]. Consequently, a challenging problem entails the development of systems for modulating the RNA activity. Development of RNA binding molecules has been critically limited in the past due to the complex structural diversity of various RNA structures on one hand and the relatively scanty high-resolution conformational information. This scenario has changed in the recent past with the high-resolution structure elucidation of number of RNAs. Conceptually, rational design of RNA binding drugs seeks a detailed fundamental knowledge of the binding affinity, specificity, selectivity mode and mechanism, of already existing compounds. Natural products in general due to their unmatched chemical diversity and biological relevance have been widely accepted as potential high quality pools in drug screening. For example recent studies have shown that protoberberine alkaloids berberine and palmatine and benzophenanthridine alkaloid sanguinarine can exercise high specificity to single stranded poly(A) molecules (Fig. 1, top panel)[16–20]. Sanguinarine binding specifically induced self structure formation in poly(A) revealing the possibility of tuning DNA structural elements by small molecules [20]. Virtually all mRNAs have a single stranded poly(A) tail at the 3′-end that participates in many biological process. The poly(A) tail is an important determinant in the maturation and stability of

Abbreviations: DNA, deoxyribonucleic acid; RNA, ribonucleic acid; poly(A), polyriboadenylic acid; P/D, nucleotide phosphate/alkaloid molar ratio; D/P, alkaloid/nucleotide phosphate molar ratio; CP, citrate phosphate; CD, circular dichroism; T_m, thermal melting temperature; ITC, isothermal titration calorimetry; DSC, differential scanning calorimetry; C_p, molar heat capacity at constant pressure; HOMO, highest occupied molecular orbital; LUMO, lowest unoccupied molecular orbital; GC, guanine–cytosine

* Corresponding author. Tel.: +91 33 2472 4049; fax: +91 33 2473 0284/5197.
E-mail address: gskumar@iicb.res.in (G.S. Kumar).

1010-6030/$ – see front matter © 2007 Elsevier B.V. All rights reserved.
doi:10.1016/j.jphotochem.2007.07.022

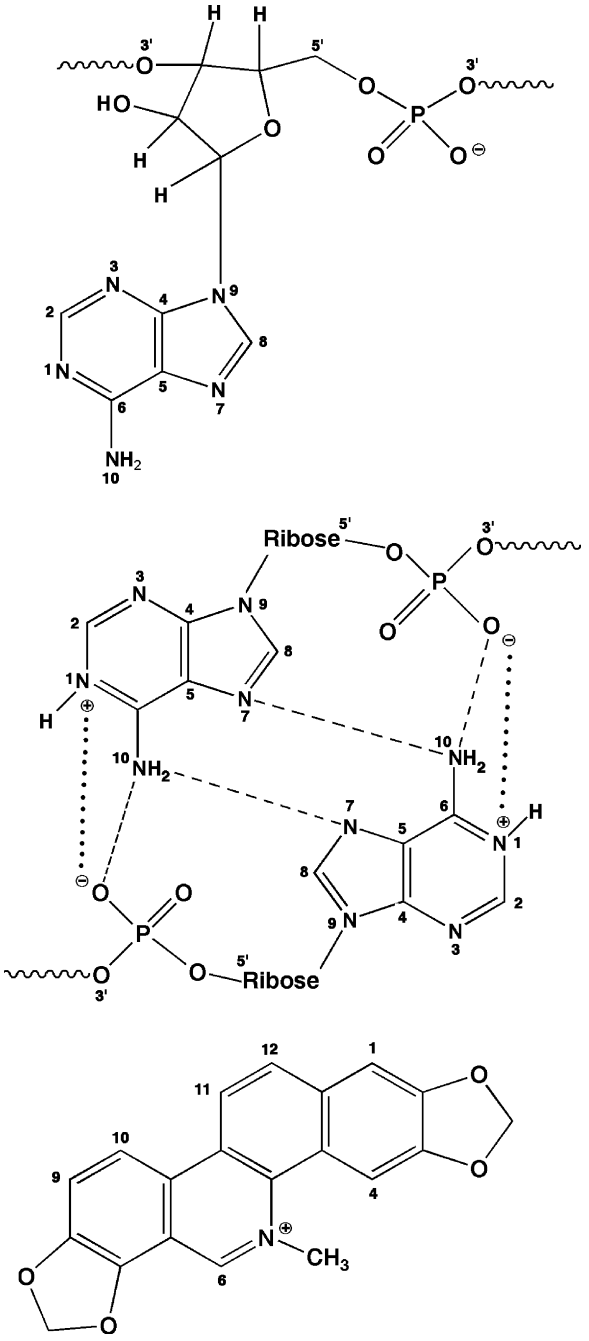

Fig. 1. Top panel: Basic structural unit of polyadenylic acid. Middle panel: Hydrogen bonding between protonated adenines (N1) in double stranded poly(AH^+). Bottom panel: Chemical structure of sanguinarine.

mRNA [21,22]. The question of formation of double helical poly(A) in eukaryotic cell has been raised recently [23] and it has been suggested that *a priori* such possibility cannot be ruled out. Adenine protonation in domain B of the hairpin ribozyme has been shown to result in the stabilization of the loop structure of the RNA enzyme [24]. In vitro, double helical poly(A) can be formed by the pairing of protonated adenines at N1 position (Fig. 1, middle panel) depending on the solution condition like pH, salt and temperature [25–29]. It has been suggested that the formation of a double helical poly(A) in the cell can terminate the polyadenylation process [23]. The study of structural and conformational transitions in poly(A) is deemed important for a better understanding of structure–function relationships in nucleic acids and also those small molecules that can bind strongly to double stranded poly(A) may be potential compounds for modulating the nucleic acid functions. Surprisingly, very few small molecules have been found to bind to double stranded poly(A) structure [30–32]. Our recent finding of self structure induction in single stranded poly(A) by sanguinarine prompted further investigations on the ability of this cytotoxic and phototoxic alkaloid to bind to double stranded poly(A) structure. Further, our long-term interest in developing anti-tumour agents from natural sources [7] led us to investigate the potential of natural compounds that could specifically target poly(A) sequences.

Sanguinarine (13-methyl benzodioxolo{5,6-c}-1,3-dioxolo{4,5-i}phenanthridinium (Fig. 1, bottom panel) is a phototoxic benzophenanthridine alkaloid derived from the root of *Sanguinaria canadenis* and other poppy-fumaria species with a long history of use world wide in folk medicine. The diverse pharmacological, photochemical and photobiological activities of sanguinarine include potent anti-microbial, anti-inflammatory, antioxidant, anticancer activities and singlet oxygen generation [33–49]. It was reported to inhibit proliferation of different types of cancer cells [50]. On the other hand, sanguinarine was found to be less toxic towards normal cells such as normal human epidermal keratinocytes [44]. Several mechanisms have been proposed to explain the antiproliforative activities of this alkaloid [46,49–52]. More recent studies correlate the cytotoxicity of sanguinarine to the DNA intercalating and subsequent ability to induce strand breaks and other DNA damaging effects [53]. In spite of a large number of studies on the interaction of sanguinarine with nucleic acids [54–59] little is known regarding its binding with RNA, particularly adenine rich RNAs and double stranded RNAs. In this paper we present detailed spectroscopic and thermodynamic elucidation of the binding of sanguinarine to double stranded poly(A).

2. Experimental

2.1. Materials

Poly (A) was purchased from Sigma–Aldrich Corporation (St. Louis, MO, USA) and used without further purification. Concentration of the sample in terms of nucleotide phosphate (hereafter nucleotide) was determined by UV absorbance measurements using molar extinction coefficient (ε) values 10,000 M^{-1} cm^{-1} at 257 nm for poly(A) [31]. Sanguinarine chloride was a product of Sigma–Aldrich and its concentration was determined by visible absorbance measurements using molar extinction coefficient $\varepsilon_{327} = 30{,}700\ M^{-1}\ cm^{-1}$ [55]. The purity of the alkaloid was tested by thin layer chromatography, melting point determination and ^1H NMR. Other reagents were of analytical grade or better. All experiments were performed in citrate–phosphate (CP) buffer containing 5 mM Na_2HPO_4, pH 4.5. pH was adjusted by citric acid. All the buffer solutions

were passed through Millipore filter of 0.45 μm to remove any particulate matter.

2.2. Methods

2.2.1. Preparation and characterization of double stranded poly(A)

The double stranded poly(A) [hereafter poly(A)] was prepared by the slow addition of single stranded poly(A) solution to CP buffer of pH 4.5 under stirring as reported earlier [17]. At least 2 h time was given for the transition to be 100% complete that was monitored by absorption and circular dichroic (CD) spectral measurements [17]. The absorption spectrum of double stranded poly(A) has a hypochromic effect (14%) compared to the single stranded spectrum (not shown). The absorption maximum of single stranded poly(A) was at 257 nm, that blue shifted to 252 nm on formation of the double stranded poly(A). The CD spectrum of the single stranded poly(A) has a strong positive band with maximum around 265 nm followed by a negative band around 210 nm while that of the double stranded poly(A) has more stronger positive band around 263 nm and a weaker negative band at 242 nm. These values are consistent to the literature data [16,17]. The double helical poly(A) was further characterized by thermal melting study and under the present conditions it melted cooperatively with a melting temperature of 65 ± 1 °C. The formation of the double stranded structure was observed to be 100% from the above characterization.

2.2.2. Preparation of sanguinarine solution

Sanguinarine is known to exist in two structurally different forms namely the low pH charged iminium form and the high pH neutral alkanolamine form [58]. The pK_a of the iminium–alkanolamine conversion under the conditions of this study was estimated to be 7.6. The charged iminium form is the biologically active form and exists 100% in the pH range 1–6 while above pH 8.5, the uncharged alkanolamine persists. So all the experiments have been performed at pH 4.5 where the structure is fully in the iminium form. The alkaloid solution was freshly prepared each day in CP buffer of pH 4.5 and kept protected until use. The alkaloid obeyed Beers law in the concentration range employed in this study.

2.2.3. Absorption spectral studies and evaluation of binding parameters

Absorption spectral titrations were performed on a Shimadzu PharmaSpec 1700 unit (Shimadzu Corporation, Kyoto, Japan) in matched quartz cells of 1 cm path length under stirring at 20 ± 0.5 °C following generally the methods described earlier [17]. A fixed concentration of poly(A) [50 μM] was titrated with increasing concentration of sanguinarine. The amount of free and bound alkaloid was determined as follows. Following each addition of the alkaloid into the polymer solution, the absorbance at the isosbestic point, 357 nm was noted (A_{obsd}) and the total alkaloid concentration present was calculated as $C_t = A_{357}/\varepsilon_{357}$. This quantity was used to calculate the expected absorbance (A^o) at the wavelength maximum, viz. 327 nm, $A^o = C_t\varepsilon_{357}$. The difference in A^o and A_{obsd} gave the bound drug concentration as

$$C_b = \frac{A}{\Delta\varepsilon} = \frac{A^\circ - A_{obsd}}{\varepsilon_f - \varepsilon_b} \quad (1)$$

where ε_f and ε_b represent the molar extinction coefficients of the free and bound sanguinarine, respectively. The free drug concentration (C_f) was determined by the difference

$$C_f = C_t - C_b \quad (2)$$

The extinction coefficient of the fully bound alkaloid was determined from the relation $\varepsilon_{b=} A_{327}/C_t$ by adding a known quantity of sanguinarine to a large excess of poly(A) assuming total binding. Alternatively, the absorbance of a known quantity of sanguinarine was monitored at 327 nm while adding known amounts of poly(A) until no further change was seen. The result of absorption titration was expressed in the form of a Scatchard plot as r/C_f versus r where r is the moles of alkaloid bound per mole of nucleotide. Non-linear Scatchard plots obtained were further analyzed by the excluded site model for non-linear non-cooperative ligand binding phenomenon using McGhee and von Hippel equation [60],

$$\frac{r}{C_f} = K'(1-nr)\left[\frac{(1-nr)}{\{1-(n-1)r\}}\right]^{(n-1)} \quad (3)$$

where K' is the intrinsic binding constant to an isolated DNA binding site, and 'n' is number of nucleotides occluded after the binding of a single alkaloid molecule. The binding data were further analyzed using the Origin 7.0 software as described earlier [61].

The spectral titration data were also analyzed by the Benesi–Hildebrand plot [62,63] by plotting the variation of C_D/ΔAbs against $1/C_S$ yielding a straight line as described previously [19]. Here, C_D and C_S denote the concentration of the alkaloid and poly(A), respectively, and ΔAbs is the difference in absorbance of free and complexed sanguinarine at 327 nm. The ratio of the intercept to slope of such plot gave K_e, the apparent equilibrium constant.

2.2.4. Continuous variation analysis (Job's plot)

To determine the binding stoichiometry of complexation of sanguinarine and poly(A). Job's continuation method [64] was applied as described previously [65]. At constant temperature, the fluorescence signal was recorded for solutions where the concentrations of both poly(A) and the alkaloid were varied while the sum of their concentration was kept constant at 50 μM. ΔF_{570} [difference in fluorescence intensity of the alkaloid in the absence and presence of poly(A) at 570 nm] was plotted as a function of the input mole fraction of sanguinarine. Break point in the resulting plot corresponds to the mole fraction of sanguinarine it the complex. The stoichiometry is obtained in terms of poly(A)–sanguinarine[$(1-\chi_{sanguinarine})/\chi_{sanguinarine}$] where $\chi_{sanguinarine}$ denotes the mole fraction of sanguinarine.

2.2.5. Circular dichroism

Circular dichroism spectra were recorded on a Jasco J715 spectropolarimeter (Japan Spectroscopic Ltd., Japan) attached

with a Jasco temperature controller and thermal programmer (model PTC 343) in rectangular quartz cells of 1 cm path length at 20 ± 0.5 °C as reported earlier [66]. Each spectrum was averaged from five successive accumulations and was base line corrected and smoothed within permissible limits using the Jasco software. The following settings were used for spectral accumulations; scan rate, 100 nm/min; bandwidth 1 nm; sensitivity, 100 milli degrees. Induced CD of sanguinarine–poly(A) complexation was measured in the region 300–550 nm by keeping a fixed concentration of the alkaloid (usually 25 μM) and varying the concentration of poly(A). The molar ellipticity values [θ] are expressed in terms of either per nucleotide (210–400 nm) or per bound alkaloid (300–550 nm).

2.2.6. Fluorescence titration and quenching studies

Steady state fluorescence measurements were performed on a Hitachi F-4010 fluorescence spectrometer (Hitachi, Tokyo, Japan) in fluorescence free quarts cells of one cm path length as described previously [67]. The excitation wavelength for sanguinarine was 475 nm and excitation and emission band pass 1.5 and 20 nm, respectively, were used throughout. All the measurements were performed at 20 ± 0.5 °C under conditions of constant stirring. The sample cell was thermostated using an Eyela unicool water bath (Tokyo Rikakikai, Japan). Uncorrected fluorescence spectra are reported.

Fluorescence quenching studies were carried out using the anionic quenchers potassium iodide (KI) and potassium ferrocyanide ($K_4Fe[CN)_6$]) at a constant molar ratio of nucleic acid to alkaloid (P/D) monitoring the fluorescence intensity changes at 570 nm as a function of the quencher concentration. At least four measurements were taken and averaged out. The data were plotted as F_o/F versus quencher concentration [Q] according to the Stern–Volmer equation, as described earlier [68].

$$\frac{F_o}{F} = 1 + K_{sv}[Q] \tag{4}$$

where F_o and F are the fluorescence intensities of the drug complex with poly(A) (P/D = 4.0) in the absence and presence of the quencher and K_{sv} is the Stern–Volmer quenching constant, which is a measure of the efficiency of the quencher.

2.2.7. Fluorescence polarization anisotropy

Fluorescence polarization anisotropy of a ligand and its complexes with nucleic acid can be given by the following expression:

$$A = \frac{I_v - I_h}{I_v + 2I_h} \tag{5}$$

where I_v and I_h are the fluorescence intensities of the vertically (v) and horizontally (h) polarized emission, when the sample is excited with vertically polarized light as described by Lakowicz [69]. I_v and I_h are obtained by placing appropriate polarizing lenses on the path of exciting and emitting light. I_v is obtained when the polarizers on the excitation and emission sides are in parallel and I_h is obtained when the polarizers are crossed at a right angle. To account for the polarization bias of the L-format single channel detection system of the fluorescence spectrometer, Eq. (5) has to be modified by introducing a polarization correction factor as follows:

$$A = \frac{I_v - GI_h}{I_v + 2GI_h} \tag{6}$$

where G is the polarization correction factor (G-factor) for the spectrometer as is defined in terms of a ratio between the vertical (I_h) (90°, 0°) and horizontal (I_v) (90°, 90°) components of fluorescence

$$G = \frac{I_h}{I_v} \tag{7}$$

In practice, fluorescence anisotropy measurements were carried out as described by Larsson et al. [70] using

$$A = \frac{I_{vv} - I_{vh}G}{I_{vv} + 2I_{vh}G} \tag{8}$$

where G is the ratio I_{hv}/I_{hh} used for instrumental correction I_{vv}, I_{vh}, I_{hv} and I_{hh} represent the fluorescence signal for excitation and emission with the polarizer set at (0°, 0°), (0°, 90°), (90°, 0°) and (90°, 90°), respectively. The samples were excited at 475 nm and the fluorescence signal was monitored at 570 nm through crossed polarizers.

2.2.8. Sensitized emission and fluorescence energy transfer

Energy transfer from base pairs to the alkaloid was studied by recording the excitation spectrum of the alkaloid in presence of poly(A) in the range 220–300 nm and verified further by sensitized emission spectra in the 500–700 nm region following the methodology reported by Kumar and co-workers [71,72].

2.2.9. Determination of fluorescence quantum efficiencies

The quantum efficiency of a nucleic acid binding ligand is a measure of the energy transferred from the nucleic acid to ligand upon complexation and is evaluated from the ratio of the quantum efficiency of ligand to nucleic acid (q_b) to the quantum efficiency of the free ligand (q_f) as given by the following equation [73]

$$Q = \frac{q_b}{q_f} = \frac{I_b}{I_f} \times \frac{\varepsilon_f}{\varepsilon_b} \tag{9}$$

where ε_f and ε_b represent the molar extinction coefficients of the free and bound sanguinarine to poly(A). ε_b was determined by titrating increasing concentrations of poly(A) to a fixed concentration of sanguinarine in 1 cm path length cell in the spectrophotometer. Each observed absorbance was subtracted from the expected absorbance of the free sanguinarine to give ΔA values. A plot of ΔA versus inverse poly(A) concentration gave an exponential plot (not shown), the y intercept of which gave the change in sanguinarine absorbance as poly(A) concentration approached infinity, i.e. the change in ligand absorbance upon reaching theoretically fully bound state. ε_b was then derived from the equation

$$\varepsilon_b = \varepsilon_f - \Delta\varepsilon \tag{10}$$

where

$$\Delta\varepsilon = \frac{\Delta A}{CI} \quad (11)$$

where C and l represent the initial ligand concentration and the path length of the cell.

2.2.10. Isothermal titration calorimetry

Isothermal titration calorimetry (ITC) was performed using a Microcal VP-ITC titration microcalorimeter (MicroCal, Inc., Northampton, MA, USA) at 20 °C as reported previously [18–20]. Degassed sanguinarine (20 μM) was placed in the calorimeter cell and poly(A) at a concentration of (3.2 mM) was added sequentially in aliquots (10 μL) from the rotating syringe (290 rpm) at 4 min intervals. Corresponding control experiments to determine the heat of dilution of the poly(A) to buffer were performed. Each injection generated a heat burst curve (microcalories per second) the area under which was determined by integration (Origin software version 7.0) that gave the measure of the heat of reaction associated with the injection. The heat associated with each poly(A)-buffer mixing was subtracted from the corresponding heat associated with the alkaloid-polynucleotide injection to give the heat of alkaloid binding for that injection. The soft ware provides the best fit values of the heat of binding (ΔH°), the stoichiometry of binding (N) and the association constant (K_a) from the plots of heat evolved per mole of poly(A) injected versus the sanguinarine molar ratio. The heat of dilution of injecting the alkaloid into the buffer alone was observed to be negligible.

2.2.11. UV optical melting study

The melting of duplex poly(A) in the absence and presence of sanguinarine was monitored using an eight cell temperature regulated cell holder in the Shimadzu Pharmaspec 1700 unit as reported previously [68]. The peltier controlled TMSPC-8 model microcell accessory (Shimadzu Corporation) allowed the collection of absorbance change over the range of temperature 10–110 °C. In a typical experiment, the poly(A) sample was mixed and diluted into the desired degassed buffer in the micro optical cuvettes of 1 cm path length and the temperature of the microcell accessory was raised at a heating rate of 0.5 °C/min while continuously monitoring the absorbance change at 252 nm. Melting curves allowed the monitoring of the hyperchromic change and estimation of melting temperature, T_m, the mid point of the hyperchromic transition.

2.2.12. Differential scanning calorimetry

Differential scanning calorimetry (DSC) measurements were performed with a Microcal VP-scanning calorimeter (MicroCal, Inc.) as reported earlier [65]. In a series of DSC scans, both the cells were loaded with buffer solution, equilibrated at 10 °C for 15 min and scanned from 10 to 115 °C at a scan rate of 50 °C/h. The buffer scans were repeated till reproducible and on cooling, the sample cell was rinsed and loaded with poly(A) and then with the poly(A)–sanguinarine complex [alkaloid/poly(A) molar ratio = 0.40] and scanned in the range 10–115 °C. The DSC thermograms of excess heat capacity versus temperature plots were analyzed using the Origin 7.1 software.

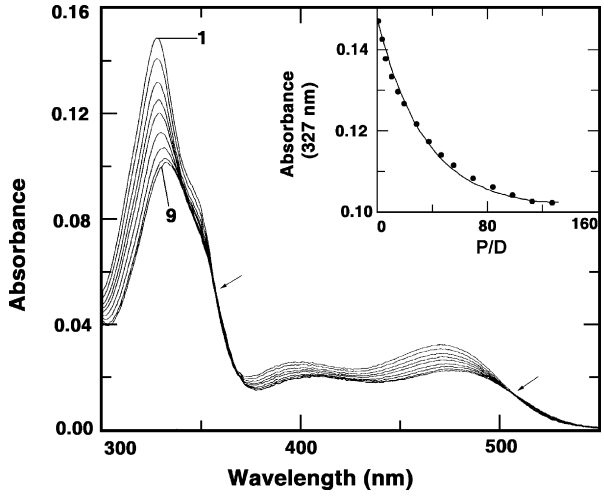

Fig. 2. Representative absorption spectral changes of sanguinarine (4.7 μM) in presence of 0, 3.57, 10.72, 19.65, 46.45, 69.67, 98.25, 113 and 141 μM (curves 1–9) of poly(A) in 10 mM CP buffer of pH 4.5 at 20 °C. *Inset*: Changes in absorbance value of sanguinarine at 327 nm with increasing P/D ratio.

3. Results and discussion

3.1. Spectrophotometric studies and elucidation of binding affinity

The binding of sanguinarine to poly(A) was studied by spectrophotometric titration. Sanguinarine has two major absorption spectral peaks in the visible region centered around 327 and 470 nm (Fig. 2). In presence of increasing concentrations of poly(A) hypochromic and bathochromic effects with isosbestic points at 357 and 507 nm were observed (marked by arrows in Fig. 2) in the sanguinarine absorbance spectrum indicating the onset of strong binding. The optical properties of sanguinarine are presented in Table 1. Such hypochromic and bathochromic effects occur due to the effective overlap of the π electron cloud of the ligand and base pairs and are suggestive of intercalative binding of sanguinarine. The sharp isosbestic points are similar to that observed with the intercalative interaction of sanguinar-

Table 1
Summary of the optical properties of free and poly(A) bound sanguinarine[a]

Absorbance	
λ_{max} (free)	327
λ_{max} (bound)	333
λ_{iso}[b]	357, 507
ε_f (at λ_{max})	30700 (327)
ε_b(at λ_{max})	17045 (327)
Fluorescence	
λ_{max} (excitation)	475
λ_{max} (emission)	570
F_o/F_b[c]	3.18

[a] Units: λ, nm; ε (molar extinction coefficient), M^{-1} cm^{-1}.
[b] Wavelengths at the isosbestic points.
[c] F_o and F_b are the fluorescence intensities of the free and completely bound sanguinarine, respectively, at 570 nm.

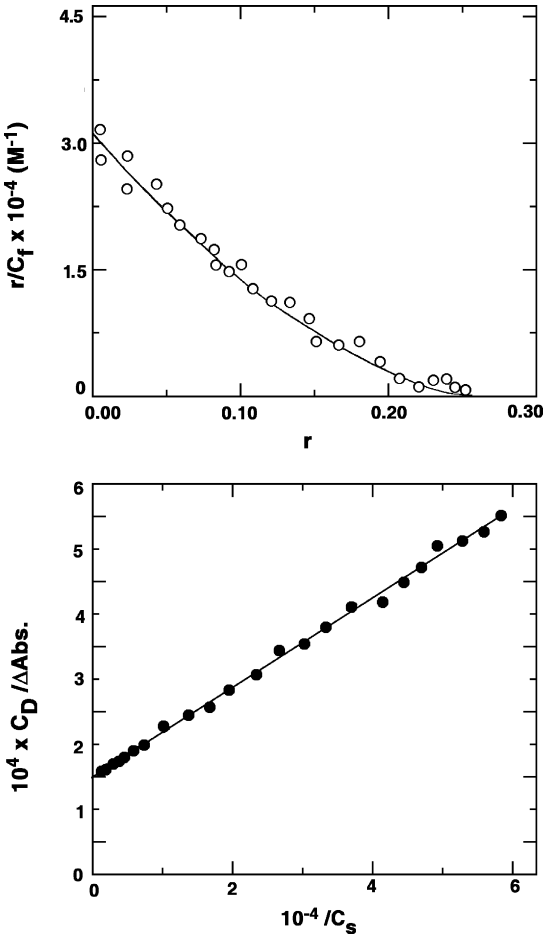

Fig. 3. Top panel: Scatchard plot of the binding of sanguinarine with poly(A). The points in the figure represent the data points and the solid line represents the best fit to the McGhee–von Hippel equation [3]. The experimental points are the average of four determinations. Bottom panel: Benesi–Hildebrand plot for poly(A)–sanguinarine complexation evaluated from spectrophotometric data at λ = 327 nm.

ine with DNA as reported previously and indicate equilibrium binding [55]. The absorbance at 327 nm decreased gradually with increasing P/D (*inset*, Fig. 2). The results of spectrophotometric titration data were expressed as Scatchard plots as well as analyzed by Benesi–Hildebrand plots. Such plots are depicted in Fig. 3. The Scatchard plot in Fig. 3 (top panel) was non-linear and concave upwards, indicating a non-cooperative binding process. The least square fitting of the Scatchard plots to the

Table 2
Summary of the binding parameters of sanguinarine to poly(A) duplex[a]

Method of analysis	Binding affinity[b] (× 10^4 M^{-1})	n[c]
McGhee–von Hippel	3.08	4.0
Benesi–Hildebrand	2.20	–
Job's method	–	4.05

[a] Average of four determinations in 10 mM in CP buffer, pH 4.5 at 20 °C.
[b] K' and K_e are is the intrinsic binding constant and the apparent equilibrium constant from the excluded site and Benesi–Hildebrand plots, respectively.
[c] n is the number of nucleotides excluded upon the binding of a single alkaloid molecule in McGhee–von Hippel analysis while the same in Job's method is the binding stoichiometry.

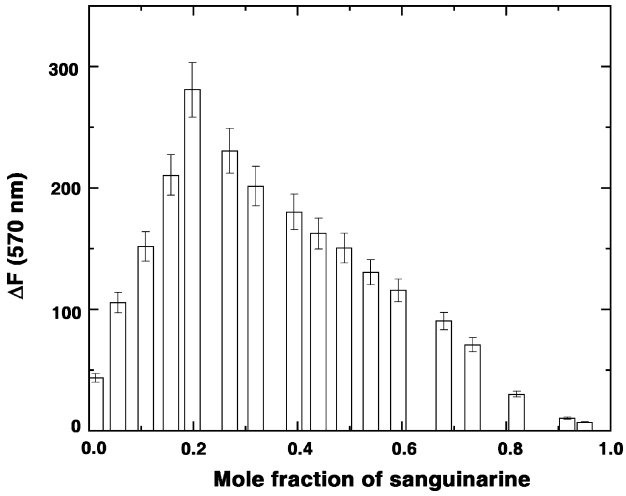

Fig. 4. Job's plot for sanguinarine binding to poly(A) in 10 mM CP buffer, pH 4.5, 20 °C.

McGhee–von Hippel equation (Eq. (3)) gave the binding affinity (K') and the number of binding sites (n) in terms of excluded sites. It was found that the binding affinity of sanguinarine to poly(A) was $3.08 \times 10^4\ M^{-1}$ with an exclusion parameter of 4 nucleotides (2 base pairs). The Benesi–Hildebrand plot (Fig. 3, bottom panel) gave a straight line with an apparent equilibrium constant (K_e) of $2.2 \times 10^4\ M^{-1}$ in agreement with the results of McGhee von Hippel analysis. The quantitative binding parameters of sanguinarine–poly(A) complexation are presented in Table 2.

3.2. Binding stoichiometry (Job's plot)

The binding stoichiometry of sanguinarine–poly(A) association and the possible number of binding sites were determined by continuous variation analysis (Job's plot) in fluorescence. The plot of difference fluorescence intensity at 570 nm versus the mole fraction of sanguinarine (Fig. 4) revealed a single binding mode for sanguinarine on poly(A). From the inflection point $\chi_{sanguinarine} = 0.198$, the number of nucleotides per sanguinarine can be estimated around 4.0 nucleotides (2 base pairs). This is in excellent agreement with the number of occluded sites obtained from the McGhee–von Hippel analysis of the spectrophotometric data.

3.3. Circular dichroic spectral study

The conformational changes associated with the binding of sanguinarine with poly(A) was probed through circular dichroic studies. The CD spectrum of poly(A) (Fig. 5, top panel) has a large positive band with maximum around 270 nm that decreased in ellipticity as the binding progressed. The association of sanguinarine to poly(A) induced optical activity in the bound molecules that has been revealed by the study of induced CD in the 300–550 nm by keeping a constant concentration of sanguinarine and varying the concentration of poly(A). Induced CD is defined as the CD of the ligand in its absorption region where the polynucleotide does not have any contribution and

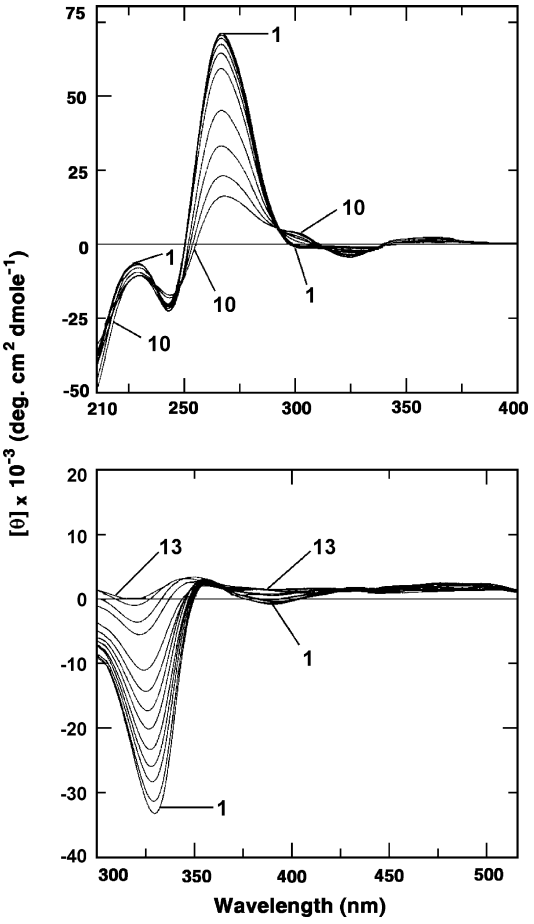

Fig. 5. Top panel: Intrinsic circular dichroic spectra of poly(A) (62 μM) with varying concentrations of 0, 3.1, 6.2, 12.4, 18.6, 24.8, 31, 37.2, 43 and 49.6 μM (curves 1–10) of sanguinarine, respectively, in 10 mM CP buffer of pH 4.5 at 20 °C. Bottom panel: Induced circular dichroic spectra of sanguinarine (25 μM) with varying concentrations of 500, 450, 400, 350, 300, 250, 200, 150, 100, 50, 37.5, 25, 18 μM of (curves 1–13) poly(A), respectively, in 10 mM CP buffer of pH 4.5 at 20 °C.

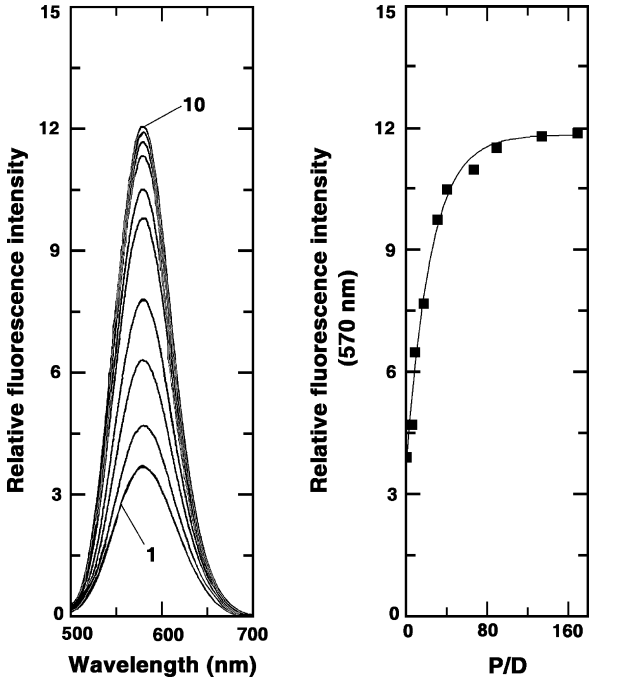

Fig. 6. Left panel: Representative steady state fluorescence emission spectrum of sanguinarine (2.4 μM, curve 1) in 10 mM CP buffer, pH 4.5 treated with 9.65, 19.30, 48.48, 72, 95.73, 168, 216, 322 and 409 μM (curves 2–10) of poly(A) at 20 °C. Right panel: Variation of steady state fluorescence intensity at 570 nm with P/D ratio.

is generated due to the asymmetric arrangement if the bound molecules on the helix. The result of such study is presented in Fig. 5 (bottom panel). An induced CD band with remarkably large negative ellipticity with peak maximum at 330 nm was observed that decreased as the P/D decreased. This study indicated the strong chiral environment of the intercalated sanguinarine in the helical organization of poly(A) and is due to the effective coupling of the transition moments of the bound sanguinarine with the transition moments of the chirally arranged base pairs.

3.4. Spectrofluorimetric titration and quenching study

Sanguinarine is a strong fluorophore that gives an emission spectrum with maximum around 570 nm when excited at 475 nm (Table 1). In Fig. 6 (left panel), the fluorescence emission spectra of sanguinarine with increasing concentrations of poly(A) is presented. Fig. 6 (right panel) shows a plot of fluorescence intensity at the λ_{max} as a function of increasing P/D. The binding tends to saturate beyond a P/D of 160. The fluorescence of sanguinarine remarkably enhanced on binding to poly(A) revealing a strong binding of the drug with the poly(A) structure.

A reliable method of studying the binding of small molecules to nucleic acids is the fluorescence quenching method [69] where the molecules bound to the surface of the helix will be accessible to the quencher while those buried by intercalation inside the helix will be protected from the quencher. Anionic quenchers like $[Fe(CN)_6]^{4-}$ or I^- will not be able to quench the fluorescence of the intercalated molecules. Consequently, the magnitude of the Stern–Volmer quenching constant (K_{sv}) of ligands that are bound intercalatively will be lower than that of the free molecules. In Fig. 7, the data on the fluorescence quenching of sanguinarine–poly(A) complex in presence of KI and $K_4[Fe(CN)_6]$ are presented. It can be seen that binding to poly(A) resulted in decreased quenching of the fluorescence quenching of sanguinarine. K_{sv} values of free sanguinarine with I^- and $[Fe(CN)_6]^{4-}$ were 98.0 and 83.7 L/mole, while those of bound were 21.8 and 13.0 L/mole. This result demonstrated that the bound sanguinarine is sequestered away from the solvent suggesting intercalative binding inside the poly(A) helix.

3.5. Fluorescence polarization anisotropy measurements

Fluorescence polarization anisotropy measurements provide evidence for the intercalative binding of drug into a duplex [74]. On intercalation of sanguinarine into the double helix its rotational motion should be restricted and as a consequence fluorescence from the bound chromophore should be polarized. In the absence of poly(A), fluorescence of sanguinarine was weakly polarized (0.018 ± 0.003) due to the rapid tumbling motion of

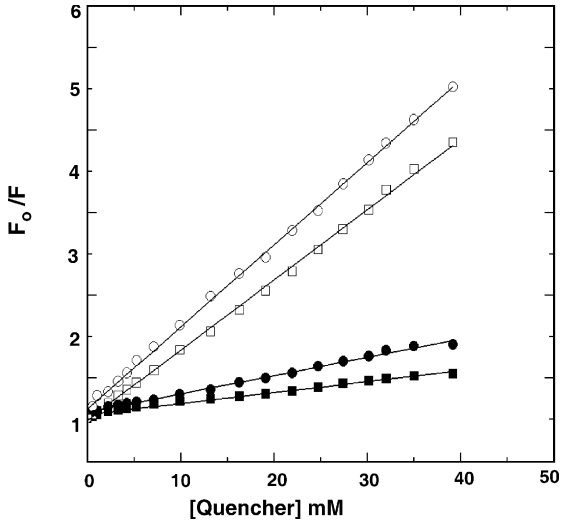

Fig. 7. Stern–Volmer plots for the quenching of sanguinarine fluorescence by KI at 20 °C in 10 mM CP buffer, pH 4.5 in the absence (◯) and in the presence of poly(A) (●) at D/P 0.40 and by $K_4[Fe(CN)_6]$ in the absence (□) and in the presence (■) of poly(A) under the same conditions.

sanguinarine in aqueous media. But on binding to poly(A) the fluorescence is significantly polarized (0.240 ± 0.002) suggesting intercalation of the alkaloid into the helix. This result is in excellent agreement with the results of quenching experiment.

3.6. Energy transfer from poly(A) bases to sanguinarine and determination of quantum efficiency

The possibility of energy transfer from the adenine bases of the duplex poly(A) to sanguinarine (Fig. 8) was explored by recording the excitation spectrum of the alkaloid in the range 210–300 nm keeping the emission fixed at 570 nm. The excitation spectrum of free sanguinarine matched excellently with the absorption spectrum (not shown). The excitation spectrum of sanguinarine–duplex poly(A) mixture resulted in intense fluorescence from sanguinarine–poly(A). The light absorption by sanguinarine in this region is minimum while poly(A) has a strong absorption band. The ratio of the excitation spectra in presence of poly(A) is shown in Fig. 9 (top panel) and this plot is an indication of direct emission from sanguinarine and values larger than one indicates sensitization by poly(A). A new band around 290 nm in the excitation spectrum in the region of absorption of poly(A) clearly indicates energy transfer from adenine base pairs to sanguinarine. The energy transfer was further confirmed by sensitized emission which is much more intense than the direct emission (Fig. 9, bottom panel).

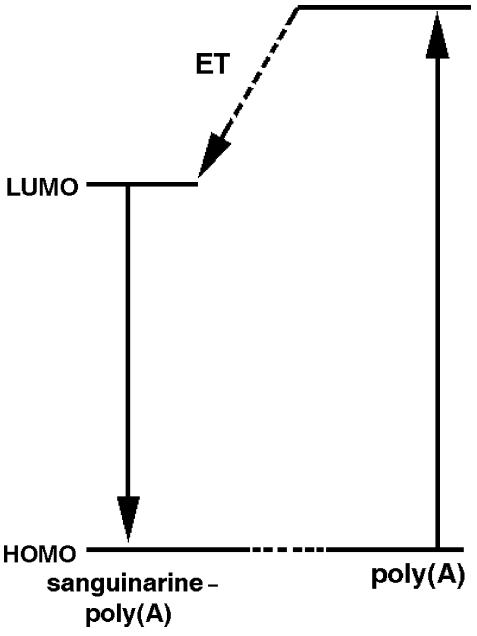

Fig. 8. Schematic energy level diagram for the energy transfer from adenine bases of poly(A) to sanguinarine.

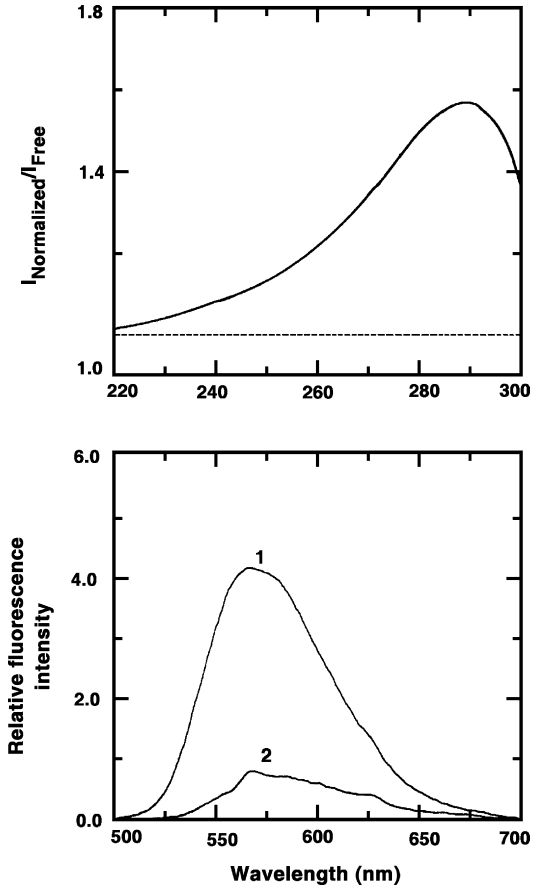

Fig. 9. Top panel: Fluorescence excitation spectra of sanguinarine recorded in the absence and presence of poly(A) in 10 mM CP buffer, pH 4.5 monitored at 570 nm at 20 °C. Bottom panel: Sensitized fluorescence spectra of sanguinarine recorded in the presence (curve 1, 290 nm excitation) and absence (curve 2) under similar condition.

Determination of quantum efficiency (Q) further supports the strong binding of sanguinarine to poly(A). A plot of ΔAbs. against the inverse of poly(A) concentration gave an exponential plot (not shown) from which a quantum efficiency value of 5.1 has been determined which indicates enhancement of the energy of the bound ligand. $Q > 1$ is indicative of enhancement of fluorescence intensity and greater retention of fluorescence energy by the bound sanguinarine due to shielding within the binding site from quenching by solvent [73].

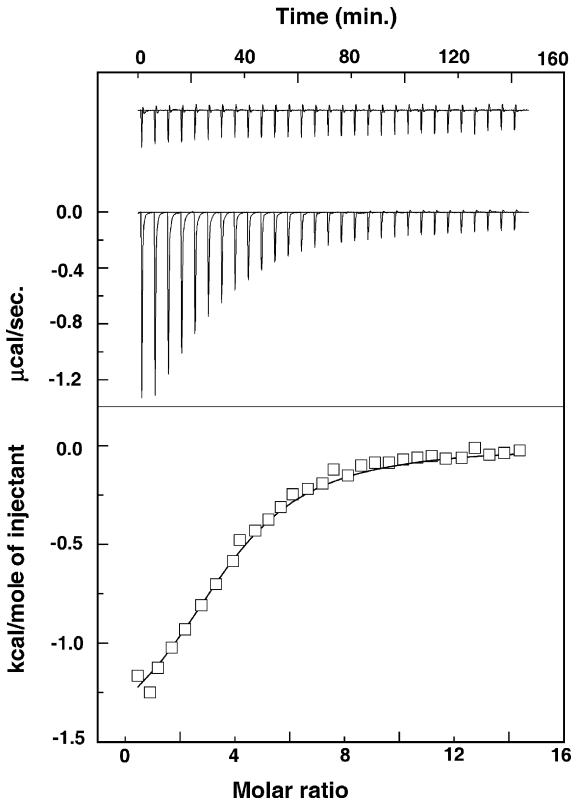

Fig. 10. Top panel: Representative ITC profile for the binding of sanguinarine to poly(A) in 10 mM CP buffer, pH 4.5 at 20 °C indicating the raw data for sequential 10 μL of 3.2 mM poly(A) into 20 μM of sanguinarine solution (curves on the bottom) and poly(A) dilution control (curves offset for clarity). Bottom panel: Plot of integrated heat data after correction of heat of dilution of poly(A) against the molar ratio of the drug to poly(A). The data (open squares) were fitted to a one-site model and the solid curve represents the best fit.

3.7. Isothermal titration calorimetry

Isothermal titration calorimetry has become an effective tool to thermodynamically characterize the binding of small molecules to macromolecules [75–76]. Further, it provides significant insight into the energetics of the complexation. Therefore, this technique was used to thermodynamically characterize the formation in poly(A)–sanguinarine complex. In Fig. 10 (top panel) the isothermal titration calorimetric data of the titration of poly(A) into a solution of sanguinarine is presented. Each injection heat burst curve in the figure corresponds to a single injection. These injection heats were corrected by subtracting the corresponding dilution heats derived from the injection of identical amounts of poly(A) into buffer alone (Fig. 10, top panel, curves off set for clarity). In Fig. 10 (bottom panel) the resulting corrected heats

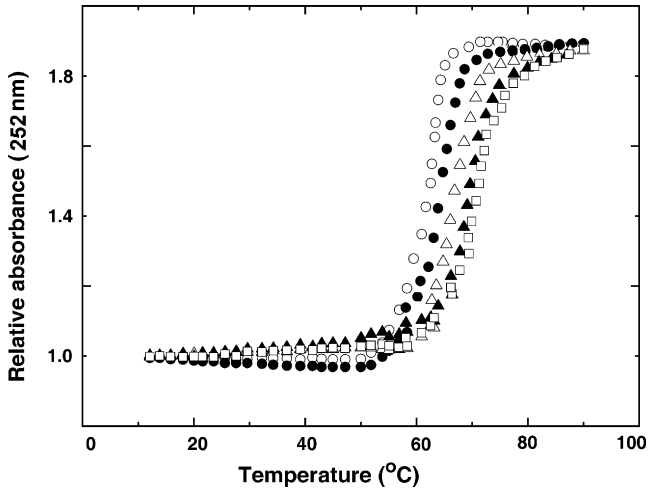

Fig. 11. Thermal melting profile of poly(A) (50 μM) treated with 0 (◯), 5 (●), 10 (△), 15 (▲), and 20 (□) μM of sanguinarine in 10 mM CP buffer, pH 4.5.

are plotted against the molar ratio. In this panel the data points reflect the experimental points while the continuous line represents the calculated fits of the data. The binding was characterized by exothermic heats. The binding affinity and thermodynamic parameters of sanguinarine–poly(A) complexation were obtained by fitting the integrated heats of association to the one site binding model to give an association constant, K_a of $7.13 \pm 0.84 \times 10^4\ M^{-1}$, which is in reasonable agreement with the spectrophotometric titration data (*vide supra*), a binding free energy (ΔG°) = -6.55 ± 1.15 kcal/mole, a $\Delta H^\circ = -5.94 \pm 1.12$ kcal/mole, a $\Delta S^\circ = 1.94 \pm 0.43$ cal/deg/mole and a binding site size (n) of about 3.7 (1/N) nucleotides (Table 3). Such negative enthalpy of binding is again generally typical for intercalative interaction of small molecules to nucleic acids [77]. The binding free energy coupled with the binding enthalpy derived from the ITC data enabled the calculation of the corresponding entropic contribution to the binding. The small entropy term, $T\Delta S^o = 0.56 \pm 0.11$ kcal/mole indicates that the binding is predominantly enthalpy driven that can be rationalized due to the formation ordered structure due to the intercalation of sanguinarine in the poly(A) helix.

3.8. Thermal melting studies

The ability of binding compounds to enhance the stability of the helix is generally studied through optical melting studies. We verified the stability enhancement of the poly(A) helix on complexation with sanguinarine. In Fig. 11, the data on the thermal melting of poly(A) with varying input ratios of sanguinarine are presented. The duplex poly(A) cooperatively melts with a T_m

Table 3
ITC derived thermodynamic profiles for the binding of sanguinarine to poly(A) duplex in 10 mM CP buffer, pH 4.5 at 20 °C[a]

T (K)	K_a ($\times 10^4\ M^{-1}$)	ΔH° (kcal/mole)	$T\Delta S^\circ$ (kcal/mole)	ΔG°(kcal/mole)	N
293	7.13 ± 0.84	-5.94 ± 1.12	0.56 ± 0.11	-6.55 ± 1.15	0.27

[a] K_a and ΔH° values were determined from fits of the ITC profiles to Origin 7.0. The values of ΔG° and $T\Delta S^\circ$ were determined using the equations $\Delta G^\circ = -(RT \ln K_a)$ and $\Delta G^\circ = \Delta H^\circ - T\Delta S^\circ$, respectively.

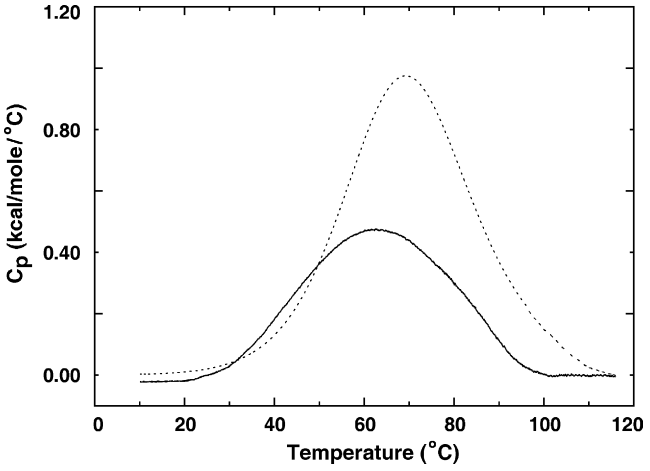

Fig. 12. DSC thermograms of poly(A) (1 mM) (solid curve) and complex of poly(A) (1 mM) and of sanguinarine (400 μM) (dotted curve) in 10 mM CP buffer, pH 4.5.

of 65 ± 1 °C that has been stabilized by the presence of bound sanguinarine. A ΔT_m of about 6 °C was obtained on saturation of the helix. This result further reiterates the strong binding of sanguinarine to poly(A).

3.9. Differential scanning calorimetry

The differential scanning calorimetry melting profiles (C_p versus T) presented in Fig. 12 further reiterate the strong binding of sanguinarine to poly(A). The melting temperature of duplex poly(A) alone (solid curve in Fig. 12) was about 65 ± 1 °C. The DSC melting of poly(A) in the absence of sanguinarine was cooperative and fully reversible enabling the application of equilibrium thermodynamics to evaluate the ratio of vant' Hoff to calorimetric enthalpy (ΔH_v = 21.22 kcal/mole, ΔH_{cal} = 21.54 kcal/mole). The ratio of the calorimetric to vant' Hoff enthalpy is unity indicating two state transition; that is, the transition occur in an all or none fashion without any intermediate state. On the other hand, in presence of the alkaloid, the stability of poly(A) enhanced with a melting temperature (T_m) of 70 ± 1 °C (dashed curve in Fig. 12) and the enthalpy of helix denaturation was several fold higher. A vant' Hoff enthalpy of 24.94 kcal/mole and a calorimetric enthalpy of 36.51 kcal/mole were evaluated from the DSC data for the sanguinarine complexed poly(A) denaturation. The melting temperature of the sanguinarine induced poly(A) complex is in complete agreement with the optical melting result.

3.10. Comparison of the binding affinity to single stranded poly(A)

The binding affinity of sanguinarine to the single stranded poly(A) has been found to be in the range (3.6–4.6) × 10^6 M^{-1} and this is about 2 orders of magnitude higher than the affinity reported here towards double stranded structure [20]. Another unique feature of the interaction to single stranded DNA was the induction of self structure in poly(A) molecules. Although the mode of interaction of sanguinarine to single and double stranded poly(A) appears to be by intercalation, the molecular aspects of the interaction like stoichiometry, energy transfer and thermodynamics appear to be significantly different.

4. Conclusions

The binding of the benzophenanthridine plant alkaloid sanguinarine to duplex poly(A) investigated by various spectroscopic and calorimetric techniques provided the following results. Sanguinarine binds strongly to the duplex poly(A) structure as evidenced by hypochromic and bathochromic effects in its absorption spectra and enhancement in its fluorescence. The binding resulted in significant polarization of the fluorescence of sanguinarine. Evidence for strong energy transfer from the poly(A) bases to the bound sanguinarine was provided further evidence for the close proximity of the bound molecules to the adenine base pairs. The stiochiometry of the binding was determined to be four nucleotides per sanguinarine. Thermodynamic parameters suggested the binding to be exothermic and enthalpy driven typical for intercalative binding. From optical and differential scanning calorimetric studies, the stability enhancement of the poly(A) helix by sanguinarine binding has been inferred. Sanguinarine is a strong GC specific DNA intercalator, and the ability of this alkaloid to intercalate and stabilize the duplex structure of poly(A) may be significant in terms of the therapeutic potential of this alkaloid.

Acknowledgements

Prabal Giri is indebted to the Council of Scientific and Industrial Research (CSIR), Government of India for the award of Junior and Senior Research Fellowships through the National Eligibility Test (NET). The authors are grateful to Prof. Siddhartha Roy, Director, Indian Institute of Chemical Biology for creating the calorimetric facility at this institute. The authors also thank all the members of the Biophysical Chemistry Laboratory, for cooperation and help at every stage of this work.

References

[1] M.J. Waring, Ann. Rev. Biochem. 50 (1981) 159–192.
[2] W.D. Wilson, Comprehensive Natural Products Chemistry, Elsevier Science, New York, 1997.
[3] J.B. Chaires, Curr. Opin. Struct. Biol. 8 (1998) 314–320.
[4] D.E. Graves, L.M. Velea, Curr. Org. Chem. 4 (2000) 915–929.
[5] G. Bischoff, S. Hoffmann, Curr. Med. Chem. 9 (2002) 312–348.
[6] R. Martinez, L.C. Garcia, Curr. Med. Chem. 12 (2005) 127–151.
[7] M. Maiti, G. Suresh Kumar, Med. Res. Rev. 27 (2007) 649–695.
[8] C.S. Chow, F.M. Bogdan, Chem. Rev. 97 (1997) 1489–1514.
[9] W.D. Wilson, K. Li, Curr. Med. Chem. 7 (2000) 73–98.
[10] J. Gallego, G. Varani, Acc. Chem. Res. 34 (2001) 836–843.
[11] E. Scholzova, R. Malík, J. Sevcik, Z. Kleibl, Cancer Lett. 246 (2007) 12–23.
[12] P. Nelson, M. Kiriakidou, A. Sharma, E. Maniataki, Z. Mourelatos, Trends Biochem. Sci. 28 (2003) 534–540.
[13] Y. Zhao, D. Srivastava, Trends Biochem. Sci. 32 (2007) 189–197.
[14] R. Niwa, F.J. Slack, Curr. Opin. Genet. Dev. 17 (2007) 145–150.
[15] C.C. Esau, B.P. Monia, Adv. Drug Deliv. Rev. 59 (2007) 101–114.
[16] R. Nandi, D. Debnath, M. Maiti, Biochim. Biophys. Acta 1049 (1990) 339–342.

[17] R.C. Yadav, G. Suresh Kumar, K. Bhadra, P. Giri, R. Sinha, S. Pal, M. Maiti, Bioorg. Med. Chem. 13 (2005) 165–174.
[18] P. Giri, M. Hossain, G. Suresh Kumar, Bioorg. Med. Chem. Lett. 16 (2006) 2364–2368.
[19] P. Giri, M. Hossain, G. Suresh Kumar, Int. J. Biol. Macromol. 39 (2006) 210–221.
[20] P. Giri, G. Suresh Kumar, Biochim. Biophys. Acta 1770 (2007) 1419–1426.
[21] M. Wickens, P. Anderson, R.J. Jackson, Curr. Opin. Genet. Dev. 7 (1997) 220–232.
[22] K. Dower, N. Kuperwasser, H. Merrikh, M. Rosbash, RNA 10 (2004) 1888–1899.
[23] M.I. Zarudnaya, D.M. Hovorun, IUBMB Life 48 (1999) 581–584.
[24] S. Ravindranathan, S.E. Butcher, J. Feigon, Biochemistry 39 (2000) 16026–16032.
[25] A. Rich, D.R. Davies, F.H. Crick, J.D. Watson, J. Mol. Biol. 3 (1961) 71–86.
[26] E. Palecek, V. Vetterl, J. Sponar, Nucleic Acids Res. 1 (1974) 427–442.
[27] W.M. Scovell, Biopolymers 17 (1978) 969–984.
[28] W. Saenger, Principles of Nucleic Acid Structure, Springer-Verlag, New York, 1984.
[29] A.G. Petrovic, P.L. Polavarapu, J. Phys. Chem. B 109 (2005) 23698–23705.
[30] T. Imae, S. Hayashi, S. Ikeda, T. Sakaki, Int. J. Biol. Macromol. 3 (1981) 259–266.
[31] C. Ciatto, M.L. D'Amico, G. Natile, F. Secco, M. Venturini, Biophys. J. 77 (1999) 2717–2724.
[32] L.M. Tumir, I. Piantanida, I.J. Cindric, T. Hrenar, Zl. Meic, M. Zinic, J. Phys. Org. Chem. 16 (2003) 891–899.
[33] G.A. Cordell, N.R. Farnsworth, Lloydia 40 (1977) 1–44.
[34] J. Lenfeld, M. Kroutil, E. Marsalek, V. Preininger, V. Simanek, Planta Med. 43 (1981) 161–165.
[35] V. Simanek, in: A. Brossi (Ed.), The Alkaloids, Academic Press Inc., London, 1985, pp. 185–240.
[36] K.C. Godowski, J. Clin. Dent. 1 (1989) 96–101.
[37] R.W. Tuveson, R.A. Larson, K.A. Marley, G.R. Wang, M.R. Barenbaum, Photochem. Photobiol. 50 (1989) 733–738.
[38] J.T. Arnason, B. Guerin, M.M. Kraml, B. Mehta, R.W. Redmond, J.C. Scaiano, Photochem. Photobiol. 55 (1992) 35–38.
[39] M. Maiti, A. Chatterjee, Curr. Sci. 68 (1995) 734–736.
[40] H. Babich, H.L. Zuckerbraun, I.B. Barber, S.B. Babich, E. Borenfreund, Pharmacol. Toxicol. 78 (1996) 397–403.
[41] T. Schmeller, B.L. Brüning, M. Wink, Phytochemistry 44 (1997) 257–266.
[42] G. Suresh Kumar, A. Das, M. Maiti, J. Photochem. Photobiol. A. Chem. 111 (1997) 51–56.
[43] M.M. Chaturvedi, A. Kumar, B.G. Darnay, G.B.N. Chainy, S. Agarwal, B.B. Aggarwal, J. Biol. Chem. 272 (1997) 30129–30134.
[44] N. Ahmad, S. Gupta, M.M Husain, K.M. Heiskanen, H. Mukhtar, Clin. Cancer Res. 6 (2000) 1524–1528.
[45] M.K. Williams, S. Dalvi, R.R. Dalvi, Vet. Hum. Toxicol. 42 (2000) 196–198.
[46] P. Weerasinghe, S. Hallock, A. Liepins, Exp. Mol. Pathol. 71 (2001) 89–98.
[47] I. Slaninova, E. Taborska, H. Bochorakova, J. Slanina, Cell. Biol. Toxicol. 17 (2001) 51–63.
[48] A. Das, A. Mukherjee, J. Chakrabarti, Mut. Res. -Gen. Toxicol. Environ. Mutagen. 563 (2004) 81–87.
[49] V.M. Adhami, M.H. Aziz, S.R. Reagan-Shaw, M. Nihal, H. Mukhtar, N. Ahmad, Mol. Can. Ther. 3 (2004) 933–940.
[50] Z. Ding, S.C. Tang, P. Weerasinghe, X. Yang, A. Pater, A. Liepins, Biochem. Pharmacol. 63 (2002) 1415–1421.
[51] J.P. Eun, G.Y. Koh, Biochem. Biophys. Res. Commun. 317 (2004) 618–624.
[52] A. Vogt, A. Tamewitz, J. Skoko, R.P. Sikorski, K.A. Giuliano, J.S. Lazo, J. Biol. Chem. 280 (2005) 19078–19086.
[53] V.O. Kaminskyy, M.D. Lootsik, R.S. Stoika, Central Eur. J. Biol. 1 (2006) 2–15.
[54] N.P.S. Bajaj, M.J. McLean, M.J. Waring, J. Mol. Recognit. 3 (1990) 48–54.
[55] A. Sen, M. Maiti, Biochem. Pharmacol. 48 (1994) 2097–2102.
[56] A. Sen, A. Ray, M. Maiti, Biophys. Chem. 59 (1996) 155–170.
[57] M. Wink, T. Schmeller, B.L. Bruning, J. Chem. Ecol. 24 (1998) 1881–1937.
[58] M. Maiti, S. Das, A. Sen, A. Das, G. Suresh Kumar, R. Nandi, J. Biomol. Struct. Dyn. 20 (2002) 455–464.
[59] L.P. Bai, Z.Z. Zhao, Z. Cai, Z.H. Jiang, Bioorg. Med. Chem. 14 (2006) 5439–5445.
[60] J.D. McGhee, P.H. von Hippel, J. Mol. Biol. 86 (1974) 469–489.
[61] K. Bhadra, M. Maiti, G. Suresh Kumar, Biochim. Biophys. Acta 1770 (2007) 1071–1080.
[62] H.A. Benesi, J.H. Hildebrand, J. Am. Chem. Soc. 71 (1949) 2703–2707.
[63] C. Yang, L. Liu, T.W. Mu, Q.X. Guo, Anal. Sci. 16 (2000) 537–539.
[64] C.Y. Huang, in: S.P. Colowick, N.O. Kaplan (Eds.), Methods in Enzymology, Academic Press, New York, 1982, pp. 509–525.
[65] Md.M. Islam, R. Sinha, G. Suresh Kumar, Biophys. Chem. 125 (2007) 508–520.
[66] R. Nandi, S. Chakraborty, M. Maiti, Biochemistry 30 (1991) 3715–3720.
[67] R. Sinha, Md.M. Islam, K. Bhadra, G. Suresh Kumar, A. Banerjee, M. Maiti, Bioorg. Med. Chem. 14 (2006) 800–814.
[68] S. Das, G. Suresh Kumar, J. Mol. Struct. 872 (2008) 56–63.
[69] J.R. Lakowicz, Principles of Fluorescence Spectroscopy, Plenum Press, New York, 1983.
[70] A. Larsson, C. Carlsson, M. Jonsson, B. Albinsson, J. Am. Chem. Soc. 116 (1994) 8459–8465.
[71] C.V. Kumar, E.H. Asuncion, J. Chem. Soc. Chem. Commun. (1992) 470–472.
[72] N.K. Modukuru, K.J. Snow, B.S. Perrin Jr., A. Bhambhani, M. Duff, C.V. Kumar, J. Photochem. Photobiol. A. Chem. 177 (2006) 43–54.
[73] N.C. Garbett, N.B. Hammond, D.E. Graves, Biophys. J. 87 (2004) 3974–3981.
[74] C.V. Kumar, E.H. Asuncion, J. Am. Chem. Soc. 115 (1993) 8547–8553.
[75] R. O' Brien, I. Haq, in: J.E. Ladbury, M. Doyle (Eds.), Biocalorimetry 2: Applications of Calorimetry in the Biological Sciences, John Wiley and Sons, West Sussex, England, 2004, pp. 3–34.
[76] J.B. Chaires, in: M. Demeunynck, C. Bailly, W.D. Wilson (Eds.), DNA and RNA Binders: From Small Molecules to Drugs, Wiley-VCH, Weinheim, 2002, pp. 461–481.
[77] J.B. Chaires, Arch. Biochem. Biophys. 453 (2006) 26–31.